

Scientific Journal of Silesian University of Technology. Series Transport

Zeszyty Naukowe Politechniki Śląskiej. Seria Transport



Volume 97

2017

p-ISSN: 0209-3324

e-ISSN: 2450-1549

DOI: <https://doi.org/10.20858/sjsutst.2017.97.2>Journal homepage: <http://sjsutst.polsl.pl>

Article citation information:

Budzik, G., Mazurkow, A. Modelling and testing of dynamic properties of C0-45 turbochargers. *Scientific Journal of Silesian University of Technology. Series Transport*. 2017, **97**, 17-25. ISSN: 0209-3324. DOI: <https://doi.org/10.20858/sjsutst.2017.97.2>.

Grzegorz BUDZIK¹, Aleksander MAZURKOW²

MODELLING AND TESTING OF DYNAMIC PROPERTIES OF C0-45 TURBOCHARGERS

Summary. The paper presents modelling process and results of the bench tests of the C0-45, which is a turbocharger for heavy-duty diesel engines. For turbochargers like this, it is necessary to measure the level of vibration. This paper presents the test results for 115 turbochargers. Rotor speed during the tests varied between 25,000 and 42,000 rpm. Rotor speed during the tests on a C0-45 turbocharger varied within three ranges, i.e., Range I: $n=25,000\div 32,000$ rpm and $a=0.5g$; Range II: $n=33,000\div 38,000$ rpm and $a=1.0g$; Range III: $n=39,000\div 42,000$ rpm and $a=1.5g$; ($g=9.81m/s^2$). Measurement of vibrations was realized by a sensor located on the body of the turbocharger. Bench tests also included measurement of key charge parameters such as the amount of mass trapped, mean flow velocities, turbulence level, gas pressure, temperature and oil flow. The results are presented in the form of diagrams showing the amplitude of the acceleration function with regard to the rotor's RPM. Research shows that using the correct parameters in construction and technological processes of assembly are very important for the effective functioning turbochargers.

Keywords: turbocharger; construction parameters; dynamic properties; level of vibration; rotor speed

¹ Department of Mechanical Engineering. Faculty of Mechanical Engineering and Aeronautics. Rzeszów University of Technology, Al. Powstańców Warszawy 8, 35-959 Rzeszów, Poland. E-mail: gbudzik@prz.edu.pl.

² Department of Mechanical Engineering. Faculty of Mechanical Engineering and Aeronautics, Rzeszów University of Technology, Al. Powstańców Warszawy 8, 35-959 Rzeszów, Poland. E-mail: almaz@prz.edu.pl.

1. INTRODUCTION

Turbochargers are mainly used to convert exhaust gases energy into compressed air energy. The air is pumped into a fuel supply system in a combustion engine.

The basic operating parameters of a turbocharger are: compression ratio, airflow, gas temperature, a maximum rotating speed and a level of vibration. The operational accuracy of a rotating set is tested with the use of an engine test stand.

2. TURBOCHARGER TEST STANDS

Each turbocharger is tested with the use of an engine test stand (Fig. 1). This facility checks the assembly quality and cooperating parts. Operational characteristics and the measurement of vibrations are also determined.

The main elements of an engine test stand are:

- turbocharger mounting brackets
- combustion chamber with a fuel system
- installation of air
- lubrication system
- measuring and control system
- exhaust system



Fig. 1. Stand test for C0-45 turbochargers and the vibration sensor

Measurement of vibrations is performed by a sensor (Fig. 1), which estimates the level of acceleration of a rotating unit system in a turbocharger. The sensor is located on the body of the turbocharger.

The level of vibrations is a basic requirement that guarantees a proper operation and the usage of a turbocharger. Measurement is performed during a set motion. Rotor speed for

a C0-45 turbocharger varies between 25,000 and 42,000 rpm. Commissioning requirements determine the values of maximal acceptable accelerations, depending on the rotating speed of a turbocharger rotor.

3. TEST STAND RESULTS

Operating parameters values for a C0-45 turbocharger are:

- compression ratio 2.8:1
- airflow $31 \div 76$ [m³/min]
- gases temperature 700 [°C]
- maximal rotating speed $n_{wmax}=42,000$ [rpm]

Values of acceptable vibrations during tests of rotating speeds for a turbocharger C0-45 are varied across three ranges:

- Range I: $25,000 \leq n_w \leq 32,000$ [rpm], $a_{dop} \leq 0.5g$
- Range II: $33,000 \leq n_w \leq 38,000$ [rpm], $a_{dop} \leq 1.0g$
- Range III: $39,000 \leq n_w \leq 42,000$ [rpm], $a_{dop} \leq 1.5g$

where $g=9.81$ m/s² equates to gravitational acceleration.

Factory acceptance tests have demonstrated that a large number of turbochargers, even when featuring suitable parameters (consumption, compression ratio), is not able to work.

During acceptance testing of 115 turbochargers, it was found that measured accelerations varied between 0.01 and 10.0 g. It should be noted that maximal acceptable accelerations can reach up to 1.5 g.

The reason why turbochargers are not used concerns excessive measured values of acceptable accelerations. Having tested all turbochargers, 33% of them do not meet the requirement concerning boundary vibration values (Fig. 2).

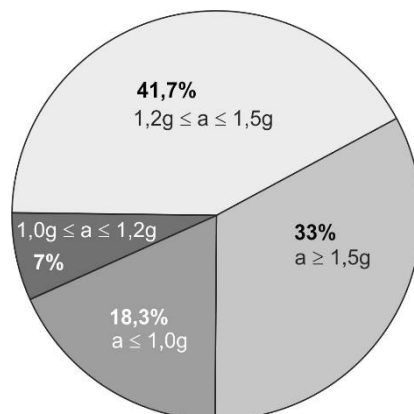


Fig. 2. Percentage of turbochargers according to vibration range level

Turbochargers that meet commissioning requirements can be divided into two groups. The first group includes turbochargers that work in upper ranges of vibrations ($0.8g < a_{dop} \leq 1.5g$) and the second group includes turbochargers that work in lower ranges

($a_{dop} \leq 0.8g$). The diagram (Fig. 3) describes vibrations in an rpm function for the first group of turbochargers, whereas the second group is presented in Fig. 4.

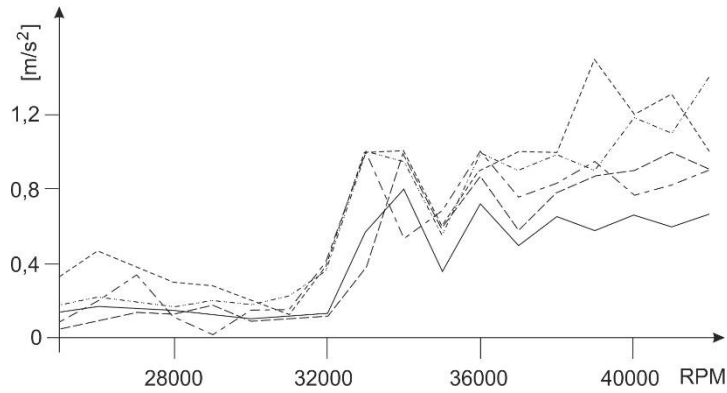


Fig. 3. Level of vibration of turbochargers ($a_{dop} \leq 1.5g$) during the rpm function

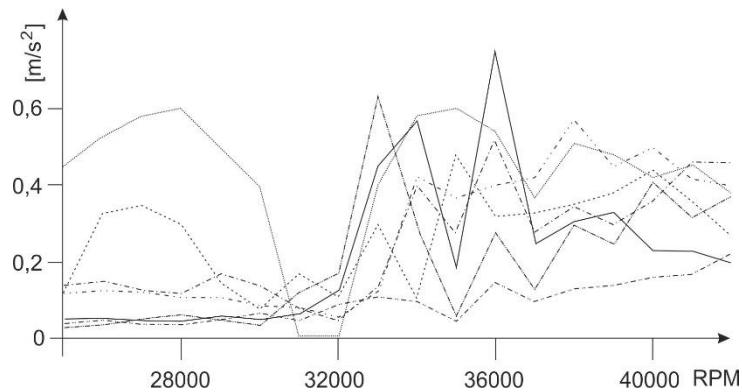


Fig. 4. Level of vibration of turbochargers ($a_{dop} \leq 0.8g$) during the rpm function

Having examined vibration measurements for the first group in the range $0 \leq n_w \leq 42,000$ rpm, we can note two resonant zones. The first zone appears during the rotating speed $n_w = 32,000$ rpm, while the second zone appears close to a speed equal to $n_w = 38,000$ rpm. Ranges of resonant zones agree with the operating ranges of turbochargers.

The second group of turbochargers features small vibrations values. In this case, there is only one resonant speed, which appears at higher rotational speeds, i.e., $n_w = 32,000 \div 37,000$ rpm.

4. ANALYSIS OF TEST STAND RESULTS

Taking into account the testing results, we can see that the right choice of construction and technological parameters of a rotating set can guarantee the correct operating parameters of turbochargers.

Turbochargers with excessive acceptable vibrations were disassembled in order to find reasons for this situation. Then, rotating units were balanced again. The assembled turbochargers were tested once more.

It was not always possible to achieve the right operating parameters of a turbocharger during another assembly because of vibrations level. Therefore, these actions were repeated to achieve the proper operating parameters.

5. THEORETICAL MODEL OF A ROTATING SET IN A TURBOCHARGER

To assure the correct work of a turbocharger, it is important to find sources of excessive vibrations and minimize them. Theoretical bases for rotor construction and explanations for vibrations in rotating sets are discussed in [1,4,7].

Test stand studies have shown that the main cause of rotational motion disturbances in a rotating set within a turbocharger is centrifugal fictitious forces, which appear because the axis of rotation does not agree with the main axis of a rotating set. These different axis locations are caused by the imbalance in rotating masses. The disequilibrium allows centrifugal fictitious forces to appear. These forces constitute outer driving forces and could lead to resonance.

It should also be mentioned that gravitational forces, which act upon rotating parts, can be the source of vibrations.

Another cause of vibrations can be related to medium resistance in the area where rotors are working.

The bearing mounting plays an essential part in rotor operations. Slide bearings with an embedded rotor could be the reason for hydrodynamic forces, which in turn contribute to self-activating vibrations in the oil layer [2,3,4,5,6,8]. In the discussed turbocharger, a rotating unit is supported in hydrodynamic bearings with a floating ring bearing.

The following reasons for vibrations have been accepted by the author for the purposes of a design model:

- imbalance in turbocharger rotors
- the mass of parts in a rotating unit
- floating ring bearing masses
- radial clearance in a lateral slide bearing with floating ring.

To explain these reasons shown above, the author has designed a dynamic model for the rotating unit of a turbocharger (Fig. 5). Rotors in a turbine and on the compressor side have different masses and different unbalance values. In this model, each bearing has been modelled, including a floating ring bearing mass. Moreover, attention has been paid to rigidity and damping factors, as well as both oil films' ability concerning vibration damping. The motion of the model is examined in two planes, i.e., OXZ and OYZ. The rigidity factors (c_x , c_y) and damping factors (d_x , d_y) are treated as coupled values.

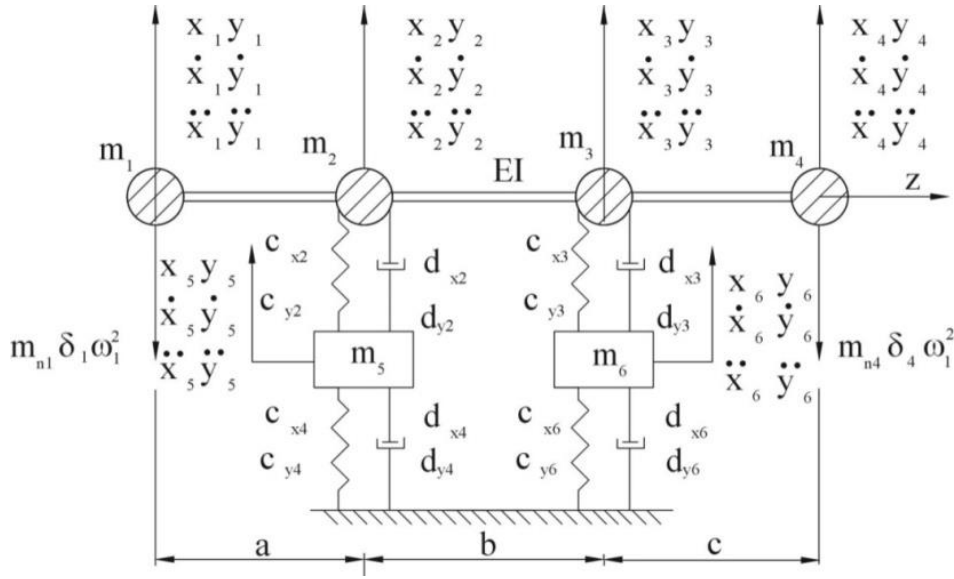


Fig. 4. Model of a rotating set

A mathematical version of the presented physics model is constituted by motion equations, which are written according to the force method for each mass of this model in planes OXZ and OYZ and can be expressed thus:

$$\begin{cases} [M_x] \cdot [\ddot{x}] + [D_{xx}] \cdot [\dot{x}] + [D_{xy}] \cdot [\dot{y}] + [C_{xx}] \cdot [x] + [C_{xy}] \cdot [y] = [F_x(t)] \\ [M_y] \cdot [\ddot{y}] + [D_{yy}] \cdot [\dot{y}] + [D_{yx}] \cdot [\dot{x}] + [C_{yy}] \cdot [y] + [C_{yx}] \cdot [x] = [F_y(t)] \end{cases} \quad (1)$$

where matrixes take the form:

$$M_x = \begin{bmatrix} M_x(1,1) & M_x(1,2) & M_x(1,3) & M_x(1,4) & 0 & 0 \\ M_x(2,1) & M_x(2,2) & M_x(2,3) & M_x(2,4) & 0 & 0 \\ M_x(3,1) & M_x(3,2) & M_x(3,3) & M_x(3,4) & 0 & 0 \\ M_x(4,1) & M_x(4,2) & M_x(4,3) & M_x(4,4) & 0 & 0 \\ 0 & 0 & 0 & 0 & M_x(5,5) & 0 \\ 0 & 0 & 0 & 0 & 0 & M_x(6,6) \end{bmatrix} \quad M_y = \begin{bmatrix} M_y(1,1) & M_y(1,2) & M_y(1,3) & M_y(1,4) & 0 & 0 \\ M_y(2,1) & M_y(2,2) & M_y(2,3) & M_y(2,4) & 0 & 0 \\ M_y(3,1) & M_y(3,2) & M_y(3,3) & M_y(3,4) & 0 & 0 \\ M_y(4,1) & M_y(4,2) & M_y(4,3) & M_y(4,4) & 0 & 0 \\ 0 & 0 & 0 & 0 & M_y(5,5) & 0 \\ 0 & 0 & 0 & 0 & 0 & M_y(6,6) \end{bmatrix}$$

$$D_{xx} = \begin{bmatrix} 0 & D_{xx}(1,2) & D_{xx}(1,3) & 0 & -D_{xx}(1,2) & -D_{xx}(1,3) \\ 0 & D_{xx}(2,2) & D_{xx}(2,3) & 0 & -D_{xx}(2,2) & -D_{xx}(2,3) \\ 0 & D_{xx}(3,2) & D_{xx}(3,3) & 0 & -D_{xx}(3,2) & -D_{xx}(3,3) \\ 0 & D_{xx}(4,2) & D_{xx}(4,3) & 0 & -D_{xx}(4,2) & -D_{xx}(4,3) \\ 0 & D_{xx}(5,2) & 0 & 0 & D_{xx}(5,5) & 0 \\ 0 & 0 & D_{xx}(6,3) & 0 & 0 & D_{xx}(6,6) \end{bmatrix} \quad D_{yy} = \begin{bmatrix} 0 & D_{yy}(1,2) & D_{yy}(1,3) & 0 & -D_{yy}(1,2) & -D_{yy}(1,3) \\ 0 & D_{yy}(2,2) & D_{yy}(2,3) & 0 & -D_{yy}(2,2) & -D_{yy}(2,3) \\ 0 & D_{yy}(3,2) & D_{yy}(3,3) & 0 & -D_{yy}(3,2) & -D_{yy}(3,3) \\ 0 & D_{yy}(4,2) & D_{yy}(4,3) & 0 & -D_{yy}(4,2) & -D_{yy}(4,3) \\ 0 & D_{yy}(5,2) & 0 & 0 & D_{yy}(5,5) & 0 \\ 0 & 0 & D_{yy}(6,3) & 0 & 0 & D_{yy}(6,6) \end{bmatrix}$$

$$D_{xy} = \begin{bmatrix} 0 & D_{xy}(1,2) & D_{xy}(1,3) & 0 & -D_{xy}(1,2) & -D_{xy}(1,3) \\ 0 & D_{xy}(2,2) & D_{xy}(2,3) & 0 & -D_{xy}(2,2) & -D_{xy}(2,3) \\ 0 & D_{xy}(3,2) & D_{xy}(3,3) & 0 & -D_{xy}(3,2) & -D_{xy}(3,3) \\ 0 & D_{xy}(4,2) & D_{xy}(4,3) & 0 & -D_{xy}(4,2) & -D_{xy}(4,3) \\ 0 & D_{xy}(5,2) & 0 & 0 & D_{xy}(5,5) & 0 \\ 0 & 0 & D_{xy}(6,3) & 0 & 0 & D_{xy}(6,6) \end{bmatrix} \quad D_{yx} = \begin{bmatrix} 0 & D_{yx}(1,2) & D_{yx}(1,3) & 0 & -D_{yx}(1,2) & -D_{yx}(1,3) \\ 0 & D_{yx}(2,2) & D_{yx}(2,3) & 0 & -D_{yx}(2,2) & -D_{yx}(2,3) \\ 0 & D_{yx}(3,2) & D_{yx}(3,3) & 0 & -D_{yx}(3,2) & -D_{yx}(3,3) \\ 0 & D_{yx}(4,2) & D_{yx}(4,3) & 0 & -D_{yx}(4,2) & -D_{yx}(4,3) \\ 0 & D_{yx}(5,2) & 0 & 0 & D_{yx}(5,5) & 0 \\ 0 & 0 & D_{yx}(6,3) & 0 & 0 & D_{yx}(6,6) \end{bmatrix}$$

$$C_{xy} = \begin{bmatrix} 1 & 0 & 0 & 0 & 0 & 0 \\ 0 & 1 & 0 & 0 & 0 & 0 \\ 0 & 0 & 1 & 0 & 0 & 0 \\ 0 & 0 & 0 & 1 & 0 & 0 \\ 0 & C_{xx}(5,2) & 0 & 0 & 1 & 0 \\ 0 & 0 & C_{xx}(6,3) & 0 & 0 & 1 \end{bmatrix} \quad C_{yx} = \begin{bmatrix} 1 & 0 & 0 & 0 & 0 & 0 \\ 0 & 1 & 0 & 0 & 0 & 0 \\ 0 & 0 & 1 & 0 & 0 & 0 \\ 0 & 0 & 0 & 1 & 0 & 0 \\ 0 & C_{yy}(5,2) & 0 & 0 & 1 & 0 \\ 0 & 0 & C_{yy}(6,3) & 0 & 0 & 1 \end{bmatrix}$$

$$C_{xy} = \begin{bmatrix} 0 & 0 & 0 & 0 & 0 & 0 \\ 0 & 0 & 0 & 0 & 0 & 0 \\ 0 & 0 & 0 & 0 & 0 & 0 \\ 0 & 0 & 0 & 0 & 0 & 0 \\ 0 & C_{xy(5,2)} & 0 & 0 & C_{xy(5,5)} & 0 \\ 0 & 0 & C_{xy(6,3)} & 0 & 0 & C_{xy(6,6)} \end{bmatrix} \quad C_{yx} = \begin{bmatrix} 0 & 0 & 0 & 0 & 0 & 0 \\ 0 & 0 & 0 & 0 & 0 & 0 \\ 0 & 0 & 0 & 0 & 0 & 0 \\ 0 & 0 & 0 & 0 & 0 & 0 \\ 0 & C_{yx(5,2)} & 0 & 0 & C_{yx(5,5)} & 0 \\ 0 & 0 & C_{yx(6,3)} & 0 & 0 & C_{yx(6,6)} \end{bmatrix}$$

$$F_x(t) = \begin{bmatrix} F_{x1}(t) \\ F_{x2}(t) \\ F_{x3}(t) \\ F_{x4}(t) \\ 0 \\ 0 \end{bmatrix} \quad F_y(t) = \begin{bmatrix} F_{y1}(t) \\ F_{y2}(t) \\ F_{y3}(t) \\ F_{y4}(t) \\ F_{y5}(t) \\ F_{y6}(t) \end{bmatrix}$$

Values describing the work of a rotating set are shown in Tab. 1. The influence of structural parameters on static and dynamic characteristics is described in Tab. 2, while Table 3 presents published results of the influence of unbalance on displacement amplitude in knots of rotating sets.

Tab. 1

Given parameters for calculations of a rotating unit

Bearing loads [N]			
F _{w=2} =400-600		F _{w=3} =370-550	
Rotational speed of a shaft [rpm]=			
n ₁ =ω ₁ /2π=300-500			
Concentrated masses in particular nodes [N·s²/m]			
m ₁ =5.0	m ₂ =0.3	m ₃ =0.25	m ₄ =2.0
Masses of floating ring bearings [N·s²/m]			
m ₅ =0.055-0.1176		m ₆ =0.055-0.1176	
Geometric parameters of rotating unit			
a=0.055 [m]	b=0.075 [m]	c=0.045 [m]	I _x =0.15·10 ⁻⁶ [m ⁴]
Material constants			
E=1.915·10 ¹¹ [N/m ²]		ISO VG 150	
Unbalance of rotating masses [N·s²]			
N _{w1} =0.18·10 ⁻⁴ , 0.88·10 ⁻⁴		N _{w4} =0.5·10 ⁻⁵	
Geometry of bearings with a floating ring			
Slide bearings width [m]			
B _{w1} =0.017		B _{w4} =0.017	
Radius of journal [m]			
(R _{J1}) _{w1} =10.82-15.82·10 ⁻³		(R _{J1}) _{w4} =10.82-15.82·10 ⁻³	
Floating ring bearing thickness [m]			
(g _p) _{w1} =2.97-12.97·10 ⁻³		(g _p) _{w4} =2.97-12.97·10 ⁻³	
Relative clearance of inner bearing [%]			
(ψ ₁) _{w1} =6.28-15.5		(ψ ₂) _{w4} =2.8-12.4	

Tab. 2
Influence of structural parameters on the operating parameters of a rotating set

Characteristics			
Static			Dynamic
$h_{1,2,\min} \downarrow$	$T_{1,2 \max} \downarrow$	$p_{1,2\max} \downarrow$	$A_p(x_5, x_6, y_5, y_6) \downarrow$
$\psi_i \downarrow$	$\psi_I \downarrow$	$\psi_i \uparrow$	$\psi_i \downarrow$
$C_R^* \downarrow$	$C_R^* \uparrow$	$C_R^* \uparrow$	$C^* \downarrow$
			$m_p \uparrow$
$B^* \downarrow$	$B^* \uparrow$	$B^* \uparrow$	$B^* \uparrow$
			$N_w \downarrow$
$T_z \uparrow$	$T_z \downarrow$	$T_z \downarrow$	

Tab. 3
The influence of unbalance on displacement amplitude in knots of rotating sets

Unbalance of rotating masses	Displacements amplitude in knots of rotating sets [m]					
	x_1	x_2	x_3	x_4	x_5	x_6
Task 1 $N_{w1}=0.18 \cdot 10^{-4}$, $N_{w4}=0.5 \cdot 10^{-5}$	$2.267 \cdot 10^{-6}$	$1.266 \cdot 10^{-6}$	$1.162 \cdot 10^{-6}$	$2.344 \cdot 10^{-6}$	$0.2682 \cdot 10^{-6}$	$0.2351 \cdot 10^{-6}$
Task 2 $N_{w1}=0.88 \cdot 10^{-4}$, $N_{w4}=0.5 \cdot 10^{-5}$	$6.908 \cdot 10^{-6}$	$6.19 \cdot 10^{-6}$	$8.431 \cdot 10^{-6}$	$13.16 \cdot 10^{-6}$	$1.577 \cdot 10^{-6}$	$2.076 \cdot 10^{-6}$
	y_1	y_2	y_3	y_4	y_5	y_6
Task 1 $N_{w1}=0.18 \cdot 10^{-4}$, $N_{w4}=0.5 \cdot 10^{-5}$	$3.641 \cdot 10^{-6}$	$3.185 \cdot 10^{-6}$	$2.971 \cdot 10^{-6}$	$3.203 \cdot 10^{-6}$	$0.5455 \cdot 10^{-6}$	$0.3799 \cdot 10^{-6}$
Task 2 $N_{w1}=0.88 \cdot 10^{-4}$, $N_{w4}=0.5 \cdot 10^{-5}$	$17.63 \cdot 10^{-6}$	$22.04 \cdot 10^{-6}$	$29.43 \cdot 10^{-6}$	$34.82 \cdot 10^{-6}$	$3.441 \cdot 10^{-6}$	$4.067 \cdot 10^{-6}$

6. CONCLUSION

Table 2 shows that the influence of structural parameters on static and dynamic characteristics can be, on the one hand, contradictory (e.g., the feed oil temperature and the minimal height of a lubricant gap) or, on the other hand, compatible (e.g., the feed oil temperature and the oil film maximum temperature).

The unbalance is an influence factor on displacement values (Table 3). In Task 1, the unbalance was $N_{w1}=0.18 \cdot 10^{-4}$ [$N \cdot s^2$]; however, in Task 2, it was $N_{w1}=0.88 \cdot 10^{-4}$ [$N \cdot s^2$]. Having compared these two tasks, it can be seen that in the Knot 4 displacements, the amplitude increases 11 times for the coordinate y_4 . The smaller values of displacements appear in Task 1.

The professional literature and published results show that vibrations appear during the construction stage, particularly during parts formation or turbocharger assembly. Subsequent research will deal with the misalignment of bearings on a turbine and the compressor side or mistakes made to the shape of bearing bushes and their influence on the level of vibrations in a rotating unit.

References

1. Bulushek Bruno. 1980. Das Schwimmbüchsenlager bei stationärem Betrieb. Doctoral thesis. Zürich: ETH. No. 6527,0000.
2. Domes Bernd. 1980. *Amplituden der Unwucht - und Selbsterregen Schwingungen Hochtouriger mit Rotierenden und nichtrotierenden Schwimmenden Büchsen.* [In German: *Amplitudes of Unbalance and Self-raising Vibrations at High Speed with Rotating and Non-rotating floating cans.*] Dissertation. Universität Karlsruhe.
3. Fink Peter.A. 1970. *Das Schwimmbüchsenlager unter instationärer Belastung.* [In German: *The Floating Bush Bearing Under Transient Load.*] Dissertation. Zurich: ETH.
4. Kiciński Jan. 2005. *Dynamika wirników i łożysk ślizgowych.* [In Polish: *Dynamics of Rotors and Plain Bearings.*] Gdańsk: Wydawnictwo Instytutu Maszyn Przepływowych PAN. ISBN 8388237063.
5. Krause Reinhold. 1987. *Experimentelle Untersuchung eines dynamisch beanspruchten Schwimmbüchsenlagers.* [In German: *Experimental Investigation of a Dynamically Loaded Swimming Pool Bearing.*] Dissertation. Zürich: ETH. DOI 10.3929/ethz-a-000403016.
6. Chin-Hsiu Li, S.H. Rohde 1980. "On steady state and dynamic performance characteristics of floating ring bearings". *ASME Journal of Lubrication Technology* 103 (3): 389-397. DOI 10.1115/1.3251687.
7. Muszyńska A. 1979. "Modelowanie wirników". [In Polish: "Rotor modelling".] IV training course from the Dynamics of Machines series, Jabłonna 5-10 Listopada 1979.
8. Zhang W. "Dynamic instability of multi-degree-of-freedom flexible rotor system due to full annular rub". In *Vibrations Rotating Machinery, International Conference, Heriot - Watt University, Edinburgh, 13-15 September 1988.*

Received 20.08.2017; accepted in revised form 11.10.2017



Scientific Journal of Silesian University of Technology. Series Transport is licensed under a Creative Commons Attribution 4.0 International License